Quantifying N_2O reduction to N_2 during denitrification in soils via isotopic mapping approach: model evaluation and uncertainty analysis

Di Wu[1,2]*, Reinhard Well[3], Laura M. Cárdenas[4], Roland Fuß[3], Dominika Lewicka-Szczebak[3], Jan Reent Köster[3], Nicolas Brüggemann[2], Roland Bol[2]

[1] Beijing Key Laboratory of Biodiversity and Organic Farming, College of Resources and Environmental Sciences, China Agricultural University, Beijing, China

[2] Institute of Bio- and Geosciences, Agrosphere (IBG-3), Forschungszentrum Jülich GmbH, 52425 Jülich, Germany

[3] Thünen Institute of Climate-Smart Agriculture, Bundesallee 65, 38116 Braunschweig, Germany

[4] Rothamsted Research, North Wyke, Okehampton EX20 2SB, UK

Keywords: Denitrification; N_2O reduction; N_2; Isotopic model

*Corresponding author: d.wu@cau.edu.cn

Abstract

The last step of denitrification, i.e. the reduction of N_2O to N_2, has been intensively studied in the laboratory to understand the denitrification process, predict nitrogen fertiliser losses, and to establish mitigation strategies for N_2O. However, assessing N_2 production via denitrification at large spatial scales is still not possible due to lack of reliable quantitative approaches. Here, we present a novel numerical "mapping approach" model using the $\delta^{15}N^{sp}/\delta^{18}O$ slope that has been proposed to potentially be used to indirectly quantify N_2O reduction to N_2 at field or larger spatial scales. We evaluate the model using data obtained from seven independent soil incubation studies conducted under a He-O_2 atmosphere. Furthermore, we analyse the contribution of different parameters to the uncertainty of the model. The model performance strongly differed between studies and incubation conditions. Re-evaluation of the previous data set demonstrated that using soils-specific instead of default endmember values could largely improve model performance. Since the uncertainty of modelled N_2O reduction was relatively high, further improvements to estimate model parameters to obtain more precise estimations remain an on-going matter, e.g. by determination of soil-specific isotope fractionation factors and isotopocule endmember values of N_2O production processes using controlled laboratory incubations. The applicability of the mapping approach model is promising with an increasing availability of real-time and field based analysis of N_2O isotope signatures.

1. Introduction

Assessing gaseous nitrogen (N) losses via denitrification from soils is crucial for improving the understanding of the microbial consumption of mineral nitrogen and closing the soil nitrogen budget on the global scale. During the denitrification process, NO_3^- is reduced to NO_2^-, and further to NO, N_2O and N_2. N_2O is the third most important greenhouse gas responsible for global warming (Bouwman et al., 2002) and the dominant stratospheric-ozone-depleting gas (Ravishankara et al., 2009). Furthermore, denitrification is a key transformation process in soils with both adverse and beneficial roles, since it is both a source and sink for N_2O, impairs the N use efficiency of agricultural crops and lowers the potential for NO_3^- leaching to aquatic systems (Conthe et al., 2019; Davidson and Seitzinger, 2006). The ratio of N_2O to N_2, however, is highly variable with different NO_3^- concentration, available carbon content and O_2 availability in soil (Blackmer and Bremner, 1978; Senbayram et al., 2012). Up to now, direct measurements of N_2 production in soils are still a great challenge even in the laboratory due to the high atmospheric N_2 background, while no successful direct N_2 emission measurement approach has been built in field studies yet. Indirect methods targeting N_2 production are problematic for a variety of reasons, e.g. the most commonly used acetylene inhibition technique is now considered unsuitable for quantifying denitrification rates mainly due to the catalytic decomposition of NO in presence of acetylene and O_2 (Terry and Duxbury, 1985; Groffman et al., 2006; Nadeem et al., 2013). Hence, there is an urgent need for new approaches to accurating estimation of N_2O to N_2 reduction that can be applied at the field scale.

Natural abundance stable isotopes analyses represent a promising tool to tackle this problem. The N_2O site preference ($\delta^{15}N^{sp}$), i.e. the difference in $\delta^{15}N$ between N_2O molecules substituted with ^{15}N at the central and the peripheral position, has been widely used during the last decade to distinguish the different sources of N_2O production pathways (+34‰ to +40‰ for nitrification

(Ni) and fungal denitrification (fD), -9‰ to +9‰ for bacterial denitrification (bD)) (Decock and Six, 2013; Toyoda et al., 2017). As the N_2O reduction to N_2 mainly involves the break of the bond between the central N (α position) and O, the remaining N_2O is being enriched simultaneously in ^{18}O and $^{15}N^{\alpha}$ (Park et al., 2011). Furthermore, the ratio between isotope effects for $^{15}N^{sp}$ and ^{18}O during N_2O reduction ($\eta_{red}{}^{15}N^{sp}/\eta_{red}{}^{18}O$) is relatively stable, and thus the $\delta^{15}N^{sp}/\delta^{18}O$ slopes can be used as an indicator for the N_2O reduction to N_2 process (Ostrom et al., 2007; Well and Flessa, 2009a; Park et al., 2011). Recently, a novel numerical mapping approach model using the $\delta^{15}N^{sp}/\delta^{18}O$ slope has been proposed to potentially be used to quantify the N_2O reduction to N_2 process (Lewicka-Szczebak et al., 2017). The principle of the model is to use a mixing equation simultaneously quantifying N_2O reduction and the partitioning of nitrification/fungal denitrification and bacterial denitrification, based on the sample position within the area enclosed by the N_2O reduction line and the mixing line in the $\delta^{15}N^{sp}/\delta^{18}O$ map (Lewicka-Szczebak et al., 2017). Compared to conventional methods such as ^{15}N labelling, the acetylene inhibition technique and the He incubation approach, the advantages of this isotopic model are that it is a non-invasive, convenient low cost method, which potentially facilitates the investigation of both laboratory incubation and field-scale experiment. This model has recently been used in a field study, where N_2O reduction was estimated based on N_2O isotopocules and uncertainty was exemplarily shown using scenarios assuming minimum and maximum of endmember values and enrichment factors (Buchen et al., 2018). However, a statistical approach to determine uncertainty based on all relevant parameters simultaneously and using not only average parameter estimates but their stochastic distributions has not yet been accomplished. Moreover, it has not yet been evaluated with data set from other studies. The aim of this study is to assess the performance of the mapping model via other studies and quantify the contribution of different parameters on overall uncertainties. We thus evaluated the mapping approach model

with data sets obtained from seven published independent soil incubation studies conducted under N_2 free helium (He) atmosphere incubation systems designed for measuring N_2O and N_2 emissions from soil. Furthermore, we conducted uncertainty analysis for two scenarios of the model in order to gain a better understanding of different parameters' contribution to uncertainty.

2. Material and methods

2.1 Model description

The principle of the model is to calculate the fraction of N_2O reduction and the N_2O fraction from bacterial denitrification based on the sample position in the $\delta^{15}N^{sp}/\delta^{18}O$ map using a mixing equation for the bacterial fraction and the Rayleigh equation for N_2O reduction. The schematic diagram of the model is given in Figure 1. The mixing line is drawn between the mean values for both $\delta^{15}N^{sp}$ and $\delta^{18}O$ of the respective process, while the reduction line is drawn based on $\eta_{red}\delta^{15}N^{sp}/\eta_{red}\delta^{18}O$ ratios (See Table 1 for the exact values and Appendix 1 for detailed calculations). Two scenarios were used separately in the mapping model: 1. Reduction-Mixing scenario (R-M): N_2O produced by bD is partially reduced to N_2, and subsequently the residual N_2O from bD is mixed with N_2O produced from Ni or fD. 2. Mixing-Reduction scenario (M-R): The N_2O produced by bD and by Ni/fD is first mixed and then the mixed N_2O is partially reduced to N_2 (see Appendix 1 for the detailed model description).

2.2 Model evaluation

The N_2O isotopocule data ($\delta^{15}N^{sp}$ and $\delta^{18}O$) for model evaluation were obtained from seven published soil incubation studies: The study of Bol et al. (2003), Meijide et al. (2010), Bergstermann et al. (2011), Köster et al. (2015) and Lewicka-Szczebak et al. (2015) were conducted at Rothamsted Research in North Wyke, Devon, UK; The study of Köster et al. (2013)

121 was conducted at Hanninghof Research Station in Dülmen, Germany; The study of Lewicka-
122 Szczebak et al. (2017) was conducted at Leibniz Centre for Agricultural Landscape Research,
123 Müncheberg, Germany. In total, we obtained 428 data points from soil incubation experiments
124 conducted under various conditions. In all these studies the N_2O isotopocule ratios were analysed
125 by Isotope Ratio Mass Spectrometry (IRMS) as described previously (Well et al., 2006; Köster et
126 al., 2013). The measured $\delta^{15}N^{sp}$ and $\delta^{18}O$ values of N_2O were used as input for the mapping
127 model, the N_2O and N_2 concentration of each isotopocule sample were used to calculate the
128 measured N_2O residual fraction (r_{N2O}), i.e. $N_2O/(N_2O+N_2)$ ratio, and thus used to compare with
129 the estimated r_{N2O}. The estimated r_{N2O} minimum value was set to 0, while the maximum value
130 was set to 1.

131 2.3 Uncertainty analysis

132 For uncertainty analysis, the two mapping model scenarios were implemented in R (*R Core*
133 *Team*, 2016). In order to derive uncertainties of parameters, a literature review was conducted,
134 taking into account previous papers summarizing the relevant parameters (Table 1). The reported
135 observed values of process-specific end members and reduction parameters were extracted (see
136 Appendix 2). The model parameters were derived from the weighted median (weighted by $1/n_i$,
137 where n_i are the number of reported values in the respective study of each value). This weighting
138 achieves equal weight for each study, regardless of how many measurements were conducted
139 within the study.

140 Three typical hypothetical test samples with different isotopocule values were then used for
141 uncertainty analysis to examine the contribution of different parameters to the whole uncertainty
142 based on both Reduction-Mixing and Mixing-Reduction scenarios: Sample 1: 20% N_2O reduction,
143 90% bD; Sample 2: 80% N_2O reduction, 90% bD; Sample 3: 50% N_2O reduction, 50% bD. The

144 test sample values were selected to cover low, medium and high reduction, as well as high and
145 medium % bD, to represent an area of the isotopocule map which contained most of the measured
146 samples of the data set, but varied in their contribution of N_2O reduction and the percentage of
147 bacterial denitrification with respect to the overall uncertainty. No minimum or maximum value
148 was set for estimated $r_{N2O.}$ As a first step, the model was applied on the test examples using the
149 median values of the parameter distributions (Table 1). The uncertainty analysis was then
150 conducted as a Monte-Carlo (MC) simulation for each test samples as follows:

151 1) The variances and the covariance of $\delta^{18}O$ and $\delta^{15}N^{sp}$ values were calculated from 17
152 repeated measurements of an N_2O standard gas (300 ppb, $\delta^{18}O$ = 40.2‰ vs SMOW, SP = -
153 2.27‰) by mass spectrometric analysis as described earlier (Lewicka-Szczebak et al., 2015),
154 in which, 100000 $\delta^{18}O$ and $\delta^{15}N^{sp}$ values were then sampled from multivariate normal
155 distributions (Genz and Bretz, 2009), with means according to the example values.

156 2) The literature endmember values for bD ($\delta^{18}O$, $\delta^{15}N^{sp}$), Ni + fD ($\delta^{18}O$, $\delta^{15}N^{sp}$) and isotopic
157 fractionation factors for reduction were then sampled pairwise with replacement (n = 100000),
158 i.e. following the bootstrap approach (Efron, 1979). Sampling of the endmember values (bD
159 and NifD) and enrichment parameters ($\eta red^{15}Nsp$ and $\eta red^{15}Nsp/\eta red^{18}O$) was conducted
160 pairwise. This was necessary to ensure that the covariance structure is reflected, since the
161 parameters of these pairs are related. During the sampling literature values were again
162 assigned probabilities $(1/n_i)/sum(1/n_i)$. This ensures that each study was equally likely to be
163 sampled from.

164 3) The result of the preceding steps was then used to calculate 100000 values of estimated
165 N_2O residual fraction (rN_2O), i.e. $N_2O/(N_2O+N_2)$ ratio, and fraction of nitrification and fungal
166 denitrification ($f_{Ni/fD}$) values for each scenario. From these values we calculated the median
167 and the 95% confidence interval, which describes the uncertainty.

3. Results

3.1 Model evaluation

The measured isotope data set for model evaluation were plotted in Fig. 2 as $\delta^{15}N^{sp}$ vs $\delta^{18}O$ values. The plot of Ni/fD and bD, the mixing line and the reduction line were drawn based on the included median literature values, with median $\delta^{18}O$ of Ni/fD = 43, bD = 10.7, median SP value of Ni/fD = 34.4, bD = -2.5, and the reduction line = 0.33 (Table 1). The values for mixing endmembers between Ni/fD and bD yield the $\delta^{15}N^{sp}/\delta^{18}O$ slope for the mixing line, while the values for reduction isotope effects yield the $\delta^{15}N^{sp}/\delta^{18}O$ slope for the reduction line. As shown in Fig. 2, the vast majority of the sample values are distributed on the right side of the median mixing line. However, at the same time there is a large number of points which fall below the median reduction line.

The relationships between measured and estimated r_{N2O} under Mixing-Reduction scenario (Appendix 3) and Reduction-Mixing scenario (Fig. 3) were similar. In order to examine the actual level of agreement between the estimated and observed data under the two scenarios, the Nash–Sutcliffe efficiency (NSE) was used (Nash and Sutcliffe, 1970):

$$NSE = 1 - \frac{\sum_{i=1}^{n}(O_i - E_i)^2}{\sum_{i=1}^{n}(O_i - O)^2} \quad (1)$$

where E_i is the estimated r_{N2O} value corresponding to the observed r_{N2O} value O_i; and O is the observed mean. In this assessment, an NSE = 1 refers to a perfect fit between estimated values and observed data, the model fits worse with decreasing NSE, whereas a negative NSE occurs when the observed mean is a better predictor than the model. The soil incubation conditions of the seven included studies were given in Table 2 and the result of the NSE determination for

these studies is demonstrated in Table 3. The estimated r_{N2O} values showed different agreements with observed values in different studies and various incubation conditions. The model values fitted relatively well with studies from Bol et al. (2003), Meijide et al. (2010), Köster et al. (2013) and Lewicka-Szczebak et al. (2017), but did not fit well with those of Bergstermann et al. (2011), Köster et al. (2015) and Lewicka-Szczebak et al. (2015). In general, Reduction-Mixing scenario showed higher NSE values compared to Mixing-Reduction scenario, except for Lewicka-Szczebak et al. (2017) with Histic Gleysol soil (Table 3).

3.2 Uncertainty analysis

The uncertainty analysis for test samples 1-3 is shown in Table 4. In general, the Reduction-Mixing scenario testing showed similar estimation outcomes with Mixing-Reduction in terms of the estimated median value. However, the variation of the median value was much larger in the Reduction-Mixing scenario than in the Mixing-Reduction. Among the three test samples, the high reduction test sample (Sample 2) showed the lowest variation. The contribution of each individual parameter on the model results and model uncertainty for the Sample 1 and Sample 3 are given in Appendix 4.

The result of the uncertainty analysis for individual parameters of Sample 2 (80% reduction, 90% bD) is, as an example, presented in Table 5. Among all parameters, the parameter of bD contributed most to the variation of the median value in both scenarios, while the measurement uncertainty of the samples had the smallest impact.

4. Discussion

4.1 Model performance and contribution to uncertainty

In our study the mapping approach model was applied using parameters based on the weighted median values reported in the current literature, showing that the goodness of fit for the N_2O residual fraction was very different among studies. One of the reasons for the different model performances were likely due to the huge uncertainty of input isotopic parameters (Table 1), which would thus greatly affect the subsequent prediction of the mapping approach model. As a result of this uncertainty, in our study some of data points are located outside the assumed boundaries defined by reduction and mixing line, which led to unrealistic estimated values of $r_{N2O}>1$ or $f_{Ni/fD}<0$. A better fit would be obtained if those out-of-range samples were not included (e.g. for Reduction-Mixing scenario NSE = 0.99 for Bol et al. (2003), NSE = 0.56 for Köster et al. (2013)). Therefore, to obtain more precise predictions of N_2O reduction, determination isotopic parameters specific for the respective measurement site using suitable laboratory incubations for individual soils appears to be necessary (e.g. Well and Flessa (2009a) and Lewicka-Szczebak et al. (2014)). Because the largest impact on overall uncertainty in estimated N_2O reduction was caused by the uncertainties of the bD endmember and of the isotopic enrichment factor of N_2O reduction parameters (Tables 4 and 5), an improved estimate of those parameters would be most pertinent in order to improve the precision of estimated N_2O reduction.

4.2 Improving model performance via specific parameter calibration

In order to demonstrate how a better model performance can be reached with parameter calibration, we reinvestigated the dataset of Lewicka-Szczebak et al. (2015) as an example by using literature median parameter or individually determined parameter. In that study, N_2 and N_2O fluxes from grassland soil mesocosms were investigated following amendment with

233 glucose/nitrate solution and at defined moisture levels and η_{red} and δ_0 had been determined by a
234 two-pool model of N_2O production and reduction (Lewicka-Szczebak et al., 2015). The first pool
235 consisted of the soil volume that was reached by the glucose/nitrate amendment and exhibited
236 very high N_2 and N_2O production rates, whereas the second pool was the remaining soil volume
237 that was not reached by this amendment and showing much lower production rates. Using
238 literature median parameter resulted in a poor agreement of calculated and measured r_{N2O} (Table
239 3). For pool 1, very significant improvement of the fit was achieved when for the bD endmember
240 $\delta_0{}^{18}O$ of 30‰ instead of the default value of 10‰ was applied, while the usage of the
241 individually determined reduction parameters ($\eta_{red}{}^{15}N^{SP}$ = -5.5‰, $\eta_{red}{}^{18}O$ = -12‰) did not make a
242 big difference (Table 6). For pool 2, no better fit was achieved with individually determined
243 reduction fractionation factors (data not shown), possibly due to very low fluxes and possibly
244 large errors in both flux and isotope measurements. The improvement in the fit for pool 1
245 reinforces the previous finding that the largest uncertainties are associated with bD endmember
246 values (Table 5). Whereas SP endmember values of bacterial denitrification show quite a stable
247 and well defined range, $\delta^{18}O$ values are more complex. Theoretically, the $\delta^{18}O$ of produced N_2O
248 depends mostly on the (often relatively stable) isotopic signature of soil water and the isotope
249 effect of O exchange, and to a lesser extent on the $\delta^{18}O$ value of the NO_3^- precursor (Lewicka-
250 Szczebak et al., 2016). It has previously been shown that while O exchange with water in soils is
251 often close to completeness (Kool et al., 2009), the conditions favouring extremely high specific
252 N_2O production rates may be associated with low O exchange, which would explain the high
253 value of the fitted $\delta_0{}^{18}O$ for the hot spot situation in pool 1 (Lewicka-Szczebak et al., 2015; Rohe
254 et al., 2017). This could also apply to some samples of our data set which were characterized by
255 quite high N_2O production rates resulting from the enhancement of denitrification by high

moisture and simultaneous amendment with nitrate and glucose (Bol et al., 2003; Meijede et al., 2010; Bergstermann et al., 2011) or by adding biogas digestate (Köster et al., 2015).

The $\delta^{18}O$ of soil H_2O is known in the range of -25 to +4‰ $_{SMOW}$ (Kool et al., 2007). Since the model results are vulnerable to the endmembers $\delta_0{}^{18}O$ values, one prerequisite for a good fit of the observed and estimated r_{N2O} by the mapping approach model would be the normalization of $\delta^{18}O$-N_2O data to $\delta^{18}O$ of soil water. Moreover, a further refinement in estimating typical $\delta^{18}O$ endmember values for N_2O from bacterial and fungal denitrification can only be reached if both the precursor values of NO_3^- and of soil water are taken into account (Rohe et al., 2017). Isotopic values of NO_3^- and H_2O were not available for the current data set except for the study of Lewicka-Szczebak et al. (2017). Taking that study as an example, after $\delta^{18}O$-N_2O correction the NSE value increased from 0.63 to 0.85 in Haplic Luvisol soil and from -3.7 to 0.65 in Histic Gleysol soil with Mixing-Reduction scenario, indicating that including $\delta^{18}O$ of NO_3^- and H_2O in future studies would further improve predictions.

Another possible reason for the different model performances was likely due to the various soil incubation conditions among included studies (Table 2). For instance, in the study of Lewicka-Szczebak et al. (2017) data were collected from laboratory soil incubations with two different soil types, a mineral soil (Haplic Luvisol) and an organic soil (Histic Gleysol). The fit was very good (NSE = 0.94 and 0.85 with Reduction-Mixing and Mixing-Reduction scenario) with mineral soil. However, much worse fits were found with organic soil in which higher contribution of fungal denitrification were identified (NSE = -3.3 for Reduction-Mixing and NSE = 0.65 for Mixing-Reduction). This is similar for other included studies, i.e. incubations with mineral soils fertilized with mineral fertiliser without C addition yielded better fits (Köster et al. 2013; Table 2), whereas those studies with organic fertiliser or glucose amendment or with organic soil generally showed

poor fits (Table 3). Adding C sources can enhance fungal biomass (Allison and Killham, 1988) or chemodenitrification (Wei et al., 2019), which may increase N_2O production from fungal denitrification or from abiotic processes and thus increase the uncertainty of the model performance, since the isotopic signature of nitrification, fungal denitrification and abiotic N_2O is still undistinguishable. Furthermore, η_{red} and δ_0 were suitable for mineral soils when the activity was not enhanced, however, hot-spots of denitrification induced by labile organic matter and the magnitude of N_2O reduction rates could significantly affect both η_{red} and δ_0. This indicates that it will be useful to determine these parameters not only for each soil individually but also for typical phases, e.g. when hot-spots of denitrification are induced by individual or combined impacts of crop residue incorporation, mineral or organic fertilisation and precipitation.

4.3 Reduction-Mixing or Mixing-Reduction?

Although in reality both Reduction-Mixing and Mixing-Reduction scenarios may occur during N_2O production and consumption processes, we speculate Reduction-Mixing scenario is more plausible than Mixing-Reduction scenario based on the knowledge that N_2O derived from bacterial denitrification is produced and reduced in anaerobic microsites, while nitrification derived N_2O is produced in aerobic domains (Butterbach-Bahl et al., 2013). This is also supported by the fact that in the present study the Reduction-Mixing scenario generally gave better prediction compared to the Mixing-Reduction scenario (Table 2). However, as indicated by the study of Lewicka-Szczebak et al. (2017) with organic soil, the Mixing-Reduction scenario may be more plausible under condition that fungal denitrification is a significant source for N_2O. In such case fungal N_2O may be also produced in anoxic microsites and undergo further reduction by bacterial denitrification, hence according to Mixing-Reduction scenario.

4.4 Possible strategy for upscaling

From these observations we conclude that estimation of r_{N2O} can be improved if specific values for η_{red} and δ_0 values are determined by experiments with simultaneous quantification of isotopocule values of N_2O and its precursors as well as N_2O reduction rates. While this has been demonstrated using laboratory incubations (Lewicka-Szczebak et al., 2017), recent progress in N_2 field flux determination (Well et al., 2019) suggests that field scale calibration is also possible. First case studies already demonstrate a successful application of the SP-$\delta^{18}O$ mapping approach on the larger spatial scale (Ibraim et al., 2019; Verhoeven et al., 2019)

Therefore, for upscaling purposes to determine N_2O reduction, we suggest to test the following strategy in future studies: (i) select and calibrate input parameters and validate the model with laboratory experiments incubating soil from the respective field site(s), then to (ii) collect soil and gas field experimental samples for analyzing isotopocules of emitted N_2O, as well as $\delta^{18}O$ of soil NO_3^- and soil water, and (iii) use that data with the model for quantifying the N_2 emission at larger spatial scales. Success will depend on the spatial variability of model parameters which is to date unknown.

It would also be interesting to use the mapping approach to assess N_2 emissions in other ecosystems, e.g. wetlands, rivers, or ocean systems, after model validation for such environments. However, it would be necessary to confirm endmember ranges and the isotope effects for these systems. Previous work suggests that due to the low diffusive isotope effects in water the O and bulk-N isotope effects of N_2O reduction in water-saturated systems like aquifers (Well et al., 2012) can be quite different from those occurring in unsaturated soils (Lewicka-Szczebak et al 2014). Moreover, SP has been shown a poor indicator for N_2O reduction in denitrifying aquifers, probably due to the complete N_2O consumption in microsites (Well et al., 2012). Nevertheless,

due to the prominent role of N_2 production in aquatic systems (Seitzinger et al., 2006), it would be worth to adapt the isotopocule mapping approach.

5. Conclusions

Our study indicated that the mapping approach model is promising to be used for indirect assessment of N_2 emission, especially at field condition where direct N_2 measurement is still not possible. Considering the fact that model performance strongly differed between the different studies and various incubation conditions, we propose at this moment the mapping approach model should not be treated as a precise quantitative tool, but would rather be an approach that yields a rough estimation of the product ratio, which is, to the best of our knowledge, not attainable with other methods until now. Future work with independent measurements of isotope effects and endmember values are also needed to constrain the large uncertainty of the model input parameters. For upscaling purposes to estimate $N_2O/(N_2O+N_2)$ ratios, we recommend that the model should only be applied after proper parameter calibration with soil incubation or field flux experiments allowing for independent determination of N_2O reduction to N_2. Nevertheless, the principles behind the mapping approach model could also be applied to assess N_2 emissions in other ecosystems, e.g. wetlands, rivers, or ocean systems, after model validation for such environments. Since the model is based on large data set of N_2O isotopocules measurements, with an increasing availability of real-time and field based data of N_2O isotope signatures (e.g. through quantum cascade laser absorption spectroscopy), the applicability of the mapping approach model can only become more widespread.

346 Acknowledgements

347 This study was supported by the National Natural Science Foundation of China (Nos.
348 41907024) , Chinese Universities Scientific Fund (2019TC152), the Deutsche
349 Forschungsgemeinschaft through the research unit DFG - FOR 2337: "Denitrification in
350 Agricultural Soils: Integrated Control and Modeling at Various Scales (DASIM)" and DFG: LE
351 3367/1-1. The authors thank Dr. Ana Meijide and Dr. Anja Sielhorst (née Bergstermann) for
352 providing N_2O isotopomer raw data.

353

References

Allison, M.F., Killham, K. 1988. Response of soil microbial biomass to straw incorporation. J. Soil Sci. 39, 237-242

Bergstermann A., Cárdenas L., Bol R., Gilliam L., Goulding K., Meijide A., Scholefield D., Vallejo A., Well R. 2011. Effect of antecedent soil moisture conditions on emissions and isotopologue distribution of N_2O during denitrification. Soil Biol. Biochem. 43, 240–250.

Blackmer A. M., Bremner J. M. 1978. Inhibitory effect of nitrate on reduction of N_2O to N_2 by soil microorganisms. Soil Biol. Biochem. 10, 187–191.

Bol R., Toyoda S., Yamulki S., Hawkins J. M. B., Cárdenas L. M., Yoshida N. 2003. Dual isotope and isotopomer ratios of N_2O emitted from a temperate grassland soil after fertiliser application. Rapid Commun. Mass Spectrom. 17, 2550–2556.

Bouwman, A.F., Boumans, L.J.M., Batjes, N.H., 2002. Emissions of N_2O and NO from fertilized fields: Summary of available measurement data. Glob. Biogeochem. Cycles 16, 1058.

Buchen, C., Lewicka‐Szczebak, D., Flessa, H., Well, R., 2018. Estimating N_2O processes during grassland renewal and grassland conversion to maize cropping using N_2O isotopocules. Rapid Communications in Mass Spectrometry 32, 1053–1067.

Butterbach-Bahl K., Baggs E. M., Dannenmann M., Kiese R., Zechmeister-Boltenstern S. 2013. Nitrous oxide emissions from soils: how well do we understand the processes and their controls? Phil Trans R Soc B 368, 20130122.

Casciotti K. L., Böhlke J. K., McIlvin M. R., Mroczkowski S. J., Hannon J. E. 2007. Oxygen Isotopes in Nitrite: Analysis, Calibration, and Equilibration. Anal. Chem. 79, 2427–2436.

Conthe, M., Lycus, P., Arntzen, M.Ø., Ramos da Silva, A., Frostegård, Å., Bakken, L.R., Kleerebezem, R., van Loosdrecht, M.C.M., 2019. Denitrification as an N_2O sink. Water Res. 151, 381–387.

Davidson, E.A., Seitzinger, S., 2006. The Enigma of Progress in Denitrification Research. Ecol. Appl. 16, 2057–2063.

Decock C., Six J. 2013. How reliable is the intramolecular distribution of ^{15}N in N_2O to source partition N_2O emitted from soil? Soil Biol. Biochem. 65, 114–127.

Frame C. H., Casciotti K. L. 2010. Biogeochemical controls and isotopic signatures of nitrous oxide production by a marine ammonia-oxidizing bacterium. Biogeosciences 7, 2695–2709.

Genz, A., Bretz, F. 2009. Computation of multivariate normal and t probabilities (Vol. 195). Springer Science & Business Media.

Groffman P. M., Altabet M. A., Böhlke J. K., Butterbach-Bahl K., David M. B., Firestone M. K., Giblin A. E., Kana T. M., Nielsen L. P., Voytek M. A. 2006. Methods for Measuring Denitrification: Diverse Approaches to a Difficult Problem. Ecol. Appl. 16, 2091–2122.

Heil J., Wolf B., Brüggemann N., Emmenegger L., Tuzson B., Vereecken H., Mohn J. 2014. Site-specific ^{15}N isotopic signatures of abiotically produced N_2O. Geochim. Cosmochim. Acta 139, 72–82.

Ibraim, E., Wolf, B., Harris, E., Gasche, R., Wei, J., Yu, L., Kiese, R., Eggleston, S., Butterbach-Bahl, K., Zeeman, M., Tuzson, B., Emmenegger, L., Six, J., Henne, S., Mohn, J., 2019. Attribution of N_2O sources in a grassland soil with laser spectroscopy based isotopocule analysis. Biogeosciences 16, 3247–3266.

Jinuntuya-Nortman M., Sutka R. L., Ostrom P. H., Gandhi H., Ostrom N. E. 2008. Isotopologue fractionation during microbial reduction of N_2O within soil mesocosms as a function of water-filled pore space. Soil Biol. Biochem. 40, 2273–2280.

Jung M.-Y., Well R., Min D., Giesemann A., Park S.-J., Kim J.-G., Kim S.-J., Rhee S.-K. 2014. Isotopic signatures of N_2O produced by ammonia-oxidizing archaea from soils. ISME J. 8, 1115–1125.

Kool, D.M., Wrage, N., Oenema, O., Dolfing, J., Groenigen, J.W.V., 2007. Oxygen exchange between (de)nitrification intermediates and H_2O and its implications for source determination of NO and N_2O: a review. Rapid Commun. Mass Spectrom. 21, 3569–3578.

Kool D. M., Müller C., Wrage N., Oenema O., Van Groenigen J. W. 2009. Oxygen exchange between nitrogen oxides and H_2O can occur during nitrifier pathways. Soil Biol. Biochem. 41, 1632–1641.

Köster J. R., Cárdenas L. M., Bol R., Lewicka-Szczebak D., Senbayram M., Well R., Giesemann A., Dittert K. 2015. Anaerobic digestates lower N_2O emissions compared to cattle slurry by affecting rate and product stoichiometry of denitrification – An N_2O isotopomer case study. Soil Biol. Biochem. 84, 65–74.

Köster J. R., Well R., Dittert K., Giesemann A., Lewicka-Szczebak D., Mühling K.-H., Herrmann A., Lammel J., Senbayram M. 2013. Soil denitrification potential and its influence on N_2O reduction and N_2O isotopomer ratios. Rapid Commun. Mass Spectrom. 27, 2363–2373.

Lewicka-Szczebak D., Well R., Köster J. R., Fuß R., Senbayram M., Dittert K., Flessa H. 2014. Experimental determinations of isotopic fractionation factors associated with N_2O production and reduction during denitrification in soils. Geochim. Cosmochim. Acta 134, 55–73.

Lewicka-Szczebak D., Well R., Bol R., Gregory A. S., Matthews G. P., Misselbrook T., Whalley W. R., Cárdenas L. M. 2015. Isotope fractionation factors controlling isotopocule signatures of soil-emitted N_2O produced by denitrification processes of various rates. Rapid Commun. Mass Spectrom. 29, 269–282.

Lewicka-Szczebak D., Dyckmans J., Kaiser J., Marca A., Augustin J. and Well R. 2016. Oxygen isotope fractionation during N_2O production by soil denitrification. Biogeosciences 13, 1129–1144.

Lewicka-Szczebak D., Augustin J., Giesemann A., Well R. 2017. Quantifying N_2O reduction to N_2 based on N_2O isotopocules – validation with independent methods (helium incubation and ^{15}N gas flux method). Biogeosciences 14, 711–732.

Maeda K., Spor A., Edel-Hermann V., Heraud C., Breuil M.-C., Bizouard F., Toyoda S., Yoshida N., Steinberg C., Philippot L. 2015. N_2O production, a widespread trait in fungi. Sci. Rep. 5, srep09697.

Meijide A., Cárdenas L. M., Bol R., Bergstermann A., Goulding K., Well R., Vallejo A., Scholefield D. 2010. Dual isotope and isotopomer measurements for the understanding of N_2O production and consumption during denitrification in an arable soil. Eur. J. Soil Sci. 61, 364–374.

Nadeem S., Dörsch P., Bakken L. R. 2013. Autoxidation and acetylene-accelerated oxidation of NO in a 2-phase system: Implications for the expression of denitrification in ex situ experiments. Soil Biol. Biochem. 57, 606–614.

Nash, J.E., Sutcliffe, J.V., 1970. River flow forecasting through conceptual models part I — A discussion of principles. J. Hydrol. 10, 282–290.

Ostrom N. E., Pitt A., Sutka R., Ostrom P. H., Grandy A. S., Huizinga K. M., Robertson G. P. 2007. Isotopologue effects during N_2O reduction in soils and in pure cultures of denitrifiers. J. Geophys. Res. Biogeosciences 2005–2012 112.

Park S., Pérez T., Boering K. A., Trumbore S. E., Gil J., Marquina S., Tyler S. C. 2011. Can N_2O stable isotopes and isotopomers be useful tools to characterize sources and microbial pathways of N_2O production and consumption in tropical soils? Glob. Biogeochem. Cycles 25, GB1001.

Ravishankara, A.R., Daniel, J.S., Portmann, R.W., 2009. Nitrous oxide (N_2O): the dominant ozone-depleting substance emitted in the 21st century. Science 326, 123–125.

Rohe L., Anderson T.-H., Braker G., Flessa H., Giesemann A., Lewicka‐Szczebak D., Wrage‐Mönnig N. and Well R. 2014. Dual isotope and isotopomer signatures of nitrous oxide from fungal denitrification‐a pure culture study. Rapid Commun. Mass Spectrom. 28, 1893–1903.

Rohe L., Well R., Lewicka-Szczebak D. 2017. Use of oxygen isotopes to differentiate between nitrous oxide produced by fungi or bacteria during denitrification. Rapid Commun. Mass Spectrom.

Seitzinger, S., Harrison, J.A., Böhlke, J.K., Bouwman, A.F., Lowrance, R., Peterson, B., Tobias, C., Drecht, G.V., 2006. Denitrification Across Landscapes and Waterscapes: A Synthesis. Ecological Applications 16, 2064–2090.

Senbayram M., Chen R., Budai A., Bakken L.,Dittert K. 2012. N_2O emission and the $N_2O/(N_2O+N_2)$ product ratio of denitrification as controlled by available carbon substrates and nitrate concentrations. Agric. Ecosyst. Environ. 147, 4–12.

Sutka R. L., Adams G. C., Ostrom N. E., Ostrom P. H. 2008. Isotopologue fractionation during N_2O production by fungal denitrification. Rapid Commun. Mass Spectrom. 22, 3989–3996.

Sutka R. L., Ostrom N. E., Ostrom P. H., Breznak J. A., Gandhi H., Pitt A. J., Li F. 2006. Distinguishing nitrous oxide production from nitrification and denitrification on the basis of isotopomer abundances. Appl. Environ. Microbiol. 72, 638–644.

Sutka R. L., Ostrom N. E., Ostrom P. H., Gandhi H., Breznak J. A. 2004. Nitrogen isotopomer site preference of N_2O produced by Nitrosomonas europaea and Methylococcus capsulatus Bath. Rapid Commun. Mass Spectrom. 18, 1411–1412.

Team, R. C. 2016. R: A language and environment for statistical computing [Computer software manual]. Vienna, Austria.

Terry R. E., Duxbury J. M. 1985. Acetylene Decomposition in Soils. Soil Sci. Soc. Am. J. 49, 90–94.

Toyoda S., Mutobe H., Yamagishi H., Yoshida N., Tanji Y. 2005. Fractionation of N_2O isotopomers during production by denitrifier. Soil Biol. Biochem. 37, 1535–1545.

Toyoda S., Yoshida N., Koba K. 2017. Isotopocule analysis of biologically produced nitrous oxide in various environments. Mass Spectrom. Rev. 36, 135–160.

Verhoeven, E., Barthel, M., Yu, L., Celi, L., Said-Pullicino, D., Sleutel, S., Lewicka-Szczebak, D., Six, J., Decock, C., 2019. Early season N_2O emissions under variable water management in rice systems: source-partitioning emissions using isotope ratios along a depth profile. Biogeosciences 16, 383–408.

Wei, J., Ibraim, E., Brüggemann, N., Vereecken, H., Mohn, J., 2019. First real-time isotopic characterisation of N_2O from chemodenitrification. Geochim. Cosmochim. Acta 267, 17–32.

Well R., Kurganova I., Lopes de Gerenyu V., Flessa H. 2006. Isotopomer signatures of soil-emitted N_2O under different moisture conditions—A microcosm study with arable loess soil. Soil Biol. Biochem. 38, 2923–2933.

Well R., Flessa H. 2009a. Isotopologue enrichment factors of N_2O reduction in soils. Rapid Commun. Mass Spectrom. 23, 2996–3002.

Well R., Flessa H. 2009b. Isotopologue signatures of N_2O produced by denitrification in soils. J. Geophys. Res. Biogeosciences 114, G02020.

Well, R., Eschenbach, W., Flessa, H., von der Heide, C., Weymann, D., 2012. Are dual isotope and isotopomer ratios of N2O useful indicators for N_2O turnover during denitrification in nitrate-contaminated aquifers? Geochimica et Cosmochimica Acta 90, 265–282.

Well, R., Burkart, S., Giesemann, A., Grosz, B., Köster, J.R. and Lewicka-Szczebak, D. (2019) Improvement of the 15N gas flux method for in situ measurement of soil denitrification and its product stoichiometry. Rapid Commun Mass Spectrom.;33:437–448

Yamazaki T., Hozuki T., Arai K., Toyoda S., Koba K., Fujiwara T., Yoshida N.2014. Isotopomeric characterization of nitrous oxide produced by reaction of enzymes extracted from nitrifying and denitrifying bacteria. Biogeosciences 11, 2679–2689.

492 **Tables**

493

494 **Table 1** Model parameters used in the mapping model. Table 1 gives the weighted median,
495 quartiles ($Q_{0.25}$ and $Q_{0.75}$), and the range of these parameter values. Data from *Rohe* et al. (2014);
496 *Maeda* et al. (2015); *Sutka* et al. (2004, 2006, 2008); *Frame and Casciotti* (2010); *Heil* et al.
497 (2014); *Jung* et al. (2014); *Yamazaki* et al. (2014); *Toyoda* et al. (2005); *Lewicka-Szczebak* et al.
498 (2014, 2016); *Jinuntuya-Nortman* et al. (2008) and *Well and Flessa* (2009a, 2009b).

499

Parameter	Min	$Q_{0.25}$	Median	$Q_{0.75}$	Max
$\delta^{18}O$ of bacterial denitrification (‰)	4.5	9.0	10.7	15.8	46.5
$\delta^{15}N^{sp}$ of bacterial denitrification (‰)	-8.7	-3.9	-2.5	0.1	8.5
$\delta^{18}O$ of fungal denitrification and nitrification (‰)	19.3	37.2	43.0	49.3	65.0
$\delta^{15}N^{sp}$ of fungal denitrification and nitrification (‰)	9.2	33.7	34.4	35.5	40.0
Reduction factor $N_2O\_N_2$ ($\eta_{red}{}^{15}N^{sp}$) (‰)	-9.4	-6.6	-5.3	-3.6	-2.1
Slope of reduction line (‰/‰)	0.11	0.29	0.33	0.41	0.55

500

501 **Table 2** Information of soil incubation conditions of the seven included studies.
502

Reference	Soil type	Water content	Incubation conditions	N addition	C addition
Bol *et al*. 2003	Dystric Gleysol	100% WHC	He (80%), O_2 (20%) (5 days)	KNO_3 75 kg N ha^{-1}	Glucose 394 kg C ha^{-1}
Meijide *et al. 2010*	Chromic Luvisol	85% WFPS	Oxic phase: He (90%), O_2 (10%) (day 1 - 11); Anoxic phase: He (100%) (day 12 - 21)	KNO_3 75 kg N ha^{-1}	Glucose 400 kg C ha^{-1}
Bergstermann *et al.* 2011	Chromic Luvisol	90% WFPS	Oxic phase: He (90%), O_2 (10%); Anoxic phase: 100% He (day 6 - 10)	KNO_3 75 kg N ha^{-1}	Glucose 400 kg C ha^{-1}
Köster *et al.2013*	Stagnic Luvisol Gleyic Podzol; Fluvimollic	65% WHC	He (100%); He (80%), O_2 (20%)	KNO_3 30 or 15 mM KNO_3 solution	*
Köster *et al.2015*	Clayey noncalcareous Pelostagnogley	90% WFPS	He (90%), O_2 (10%)	Anaerobic digestates and Cattle slurry; equiv to 160 kg N ha^{-1}	*
Lewicka-Szczebak *et al.2015*	Silty clay loam soil	100% WFPS 94% WFPS 85% WFPS	He (79%), O_2 (21%)	KNO_3 75 kg N ha^{-1}	Glucose 400 kg C ha^{-1}
Lewicka-Szczebak *et al. 2017*	Haplic Luvisol; Histic Gleysol	70% WFPS 80% WFPS; 75% WFPS 85%WFPS	He (80%), O_2 (20%); He (100%)	$NaNO_3$ 50 or 80 mg N kg $soil^{-1}$	*

503

504 **Table 3** Nash–Sutcliffe efficiency (NSE) of "Reduction-Mixing scenario" and "Mixing-
505 Reduction scenario" for the individual studies.

Reference	Bol et al. 2003	Meijide et al. 2010	Bergstermann et al. 2011	Köster et al. 2013	Köster et al. 2015	Lewicka-Szczebak et al. 2015	Lewicka-Szczebak et al. 2017 with Haplic Luvisol soil	Lewicka-Szczebak et al. 2017 with Histic Gleysol soil
Redcution-Mixing	0.56	0.39	0.21	0.43	0.11	0.01	0.94	-3.28
Mixing-Reduction	0.51	0.36	0.14	-0.31	-0.01	0.1	0.65	0.85

506

507

508 **Table 4** Uncertainty analysis for Sample 1-3 under "Mixing-Reduction scenario" and
509 "Reduction-Mixing scenario". "med" denotes median value, "lwr" is lower limit and "upr" is
510 upper limit of the 95 % confidence interval.

511

Sample	Scenario	True r_{N2O} values	Modelled r_{N2O} med (lwr, upr)	True $f_{Ni/fD}$ values	Modelled $f_{Ni/fD}$ med (lwr, upr)
Sample1	Reduction-Mixing	0.8	0.82 (0.1, 31.45)	0.1	0.11 (-0.24, 0.48)
	Mixing-Reduction		0.77 (0.22, 7.07)		0.11 (-0.31, 0.49)
Sample2	Reduction-Mixing	0.2	0.19 (0.00, 2.47)	0.1	0.11 (-0.23, 0.48)
	Mixing-Reduction		0.21 (0.01, 1.38)		0.12 (-0.55, 0.45)
Sample3	Reduction-Mixing	0.5	0.57 (0.02, 2810)	0.5	0.52 (0.30, 0.89)
	Mixing-Reduction		0.53 (0.14, 3.54)		0.52 (0.21, 0.97)

512

513 **Table 5** Uncertainty analysis for individual parameters of Sample 2 under "Mixing-Reduction
514 scenario" and "Reduction-Mixing scenario". "med" denotes median value, "lwr" is lower limit
515 and "upr" is upper limit of the 95 % confidence interval, "IRMS" denotes "Isotope Ratio Mass
516 Spectrometry".

Uncertainty	Scenario	r_{N2O} med (lwr, upr)	$f_{Ni/fD}$ med (lwr, upr)
bD parameter	Reduction-Mixing	0.16 (0.12, 1.37)	0.10 (-0.21, 0.41)
	Mixing-Reduction	0.20 (0.08, 1.21)	0.10 (-0.21, 0.41)
Ni/fD parameter	Reduction-Mixing	0.17 (0.14, 0.21)	0.10 (0.08, 0.18)
	Mixing-Reduction	0.20 (0.18, 0.27)	0.10 (0.08, 0.18)
Reduction parameter	Reduction-Mixing	0.17 (0.00, 0.47)	0.10 (0.01, 0.18)
	Mixing-Reduction	0.19 (0.03, 0.36)	0.10 (-0.21, 0.27)
IRMS measurement	Reduction-Mixing	0.17 (0.16, 0.17)	0.10 (0.06, 0.14)
	Mixing-Reduction	0.20 (0.18, 0.22)	0.10 (0.06, 0.14)

517

518

519 **Table 6** Comparison of model performance between default parameter and calibrated parameter
520 input for the study of *Lewicka-Szczebak* et al. (2015) by using Nash–Sutcliffe efficiency (NSE).
521 Information for default parameter can be found in Table 1, while calibrated parameter is $\eta_{red}{}^{15}N^{sp}$ =
522 -5.5; $\eta_{red}{}^{18}O$ = -12‰; $\delta\ ^{18}O$ of bD = 30‰.

Scenario	Model with default parameter	Model with calibrated parameter
Reduction-Mixing	-0.59	0.62
Mixing-Reduction	-0.93	0.59

523

524

Figures

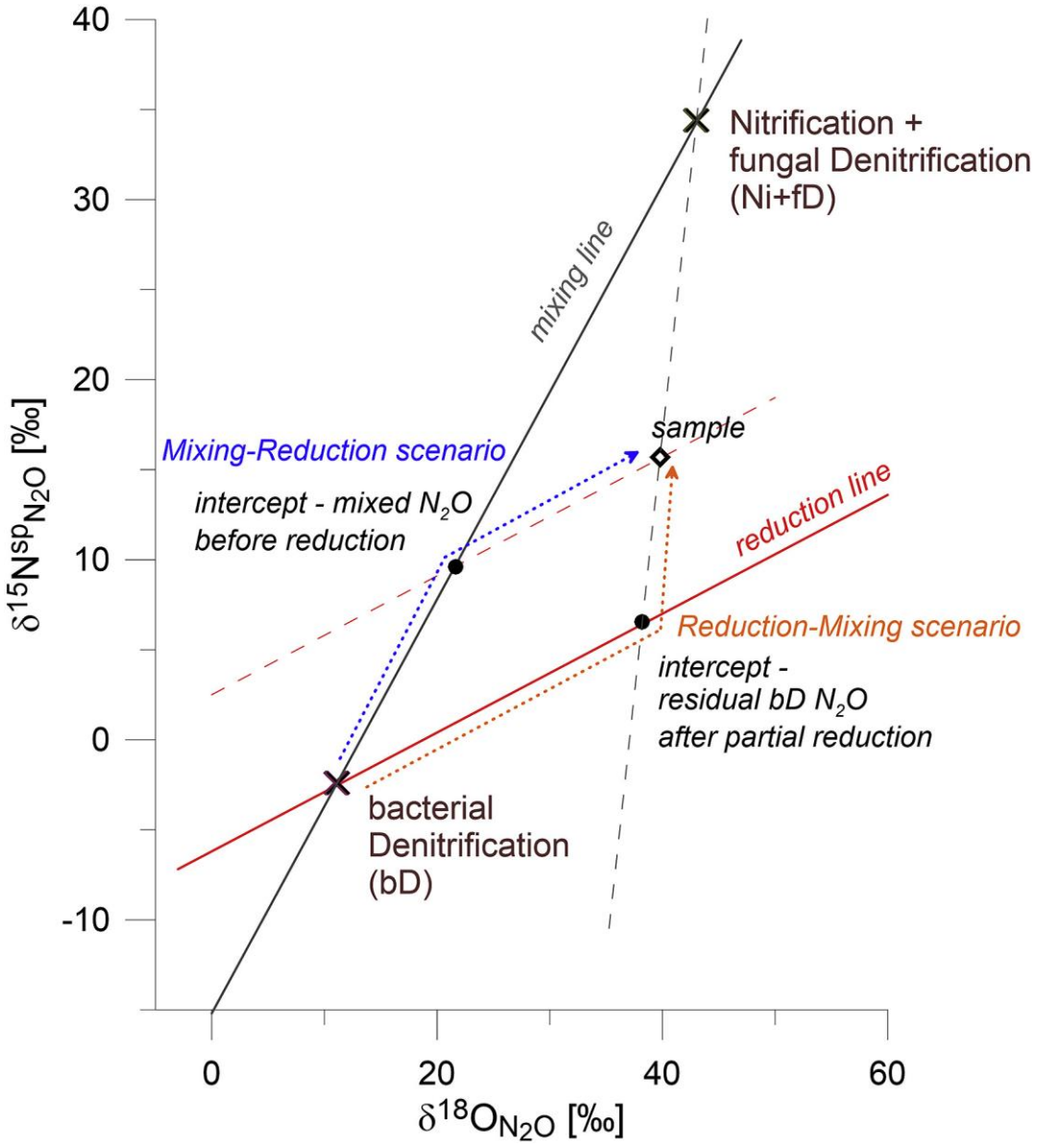

Figure 1 Schematic diagram of the mapping approach to illustrate the simultaneous estimation of N_2O reduction and the contribution of different processes to soil-emitted N_2O (modified after *Lewicka-Szczebak* et al., 2017 and *Buchen et al*., 2018). For mixing endmembers (bD and Ni+fD) median values are presented. Dotted lines illustrate the combination of N_2O mixing and reduction assumed in the calculations, where orange dotted line represents Reduction-Mixing scenario, and blue dotted line represents Mixing-Reduction scenario (see 2.1 model description).

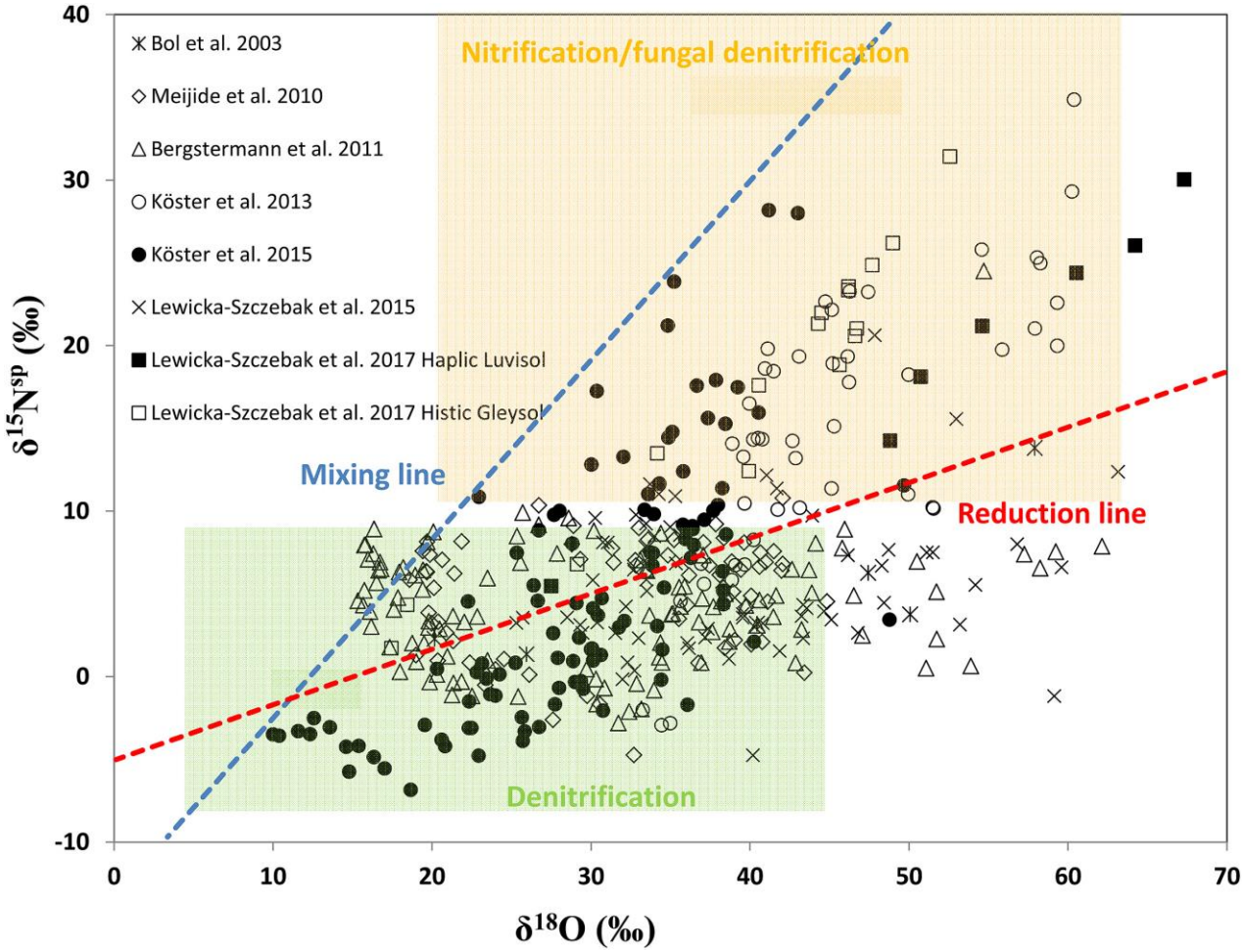

533

534 **Figure 2** The position of included data points in the mapping approach map. The plot of Ni/fD
535 and bD, the reduction line and mixing line were drawn based on the included median literature
536 values. The light color square area indicates the Min and Max of input parameter, while the deep
537 color square area indicates $Q_{0.25}$ and $Q_{0.75}$ values of end member parameter, according to literature
538 values.

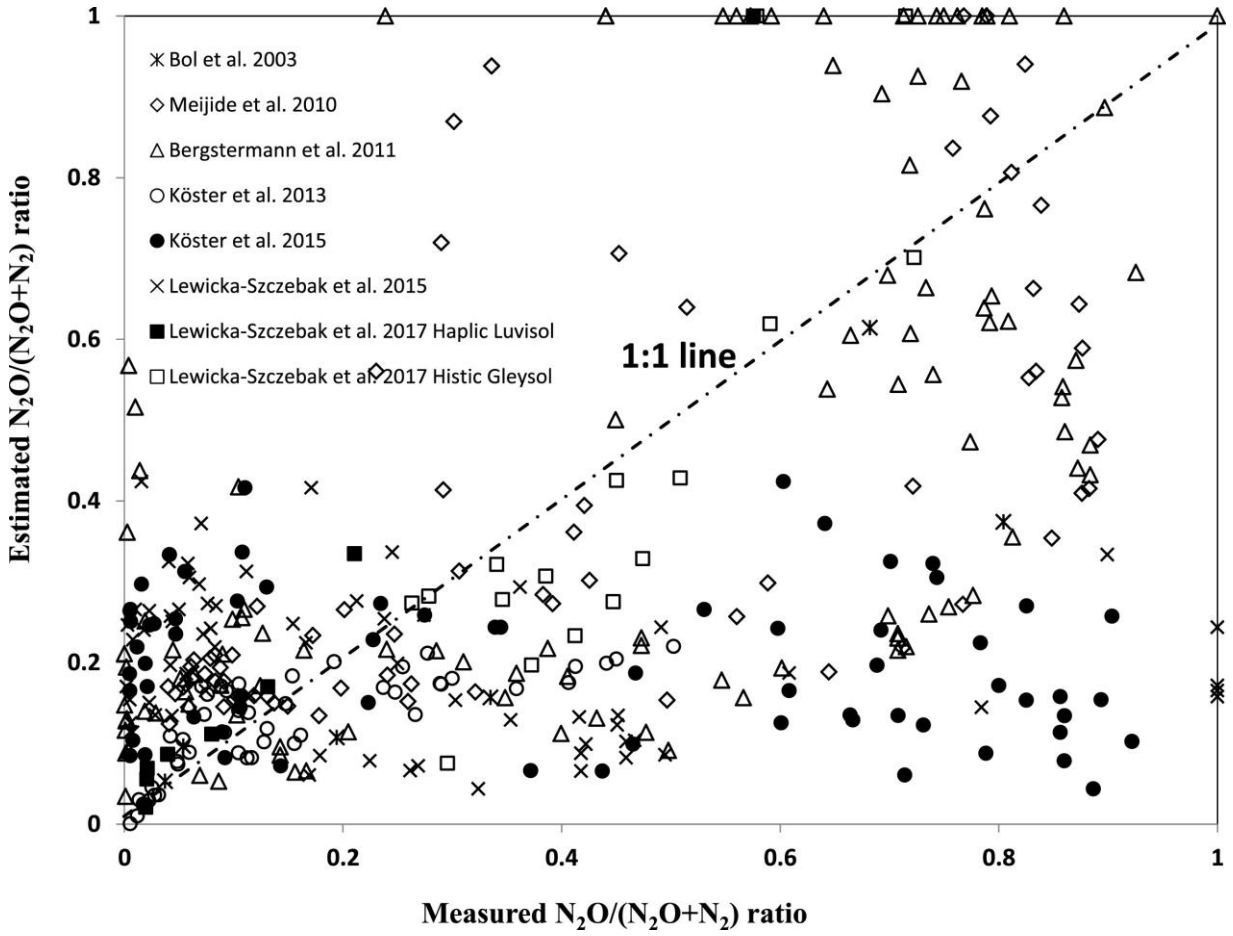

539

540 **Figure 3** Observed and estimated $N_2O/(N_2O+N_{2)}$ ratio (r_{N2O}) with Reduction-Mixing scenario.